Supplementary information

Dimensional tunability and photoluminescence triggered by solvent encapsulation strategies in hybrid materials

Bo Zhuang,[a] Qiang-Qiang Jia,[b] Zhi-Long Li,[a] Jiu-Yang Liu,[a] Ying Wang,[a] Jia-Xun Li,[a] Kun Ding, *[a] Zun-Qi Liu*[c] and Da-Wei Fu*[b,c]

[a] Ordered Matter Science Research Center, Jiangsu Key Laboratory for Science and Applications of Molecular Ferroelectrics, Southeast University, Nanjing 211189, P. R. China.

[b] Institute for Science and Applications of Molecular Ferroelectrics, Key Laboratory of the Ministry of Education for Advanced Catalysis Materials, Zhejiang Normal University, Jinhua, 321004, P. R. China.

[c] Chemistry and Chemical Engineering College, Xinjiang Agricultural University, Urumqi 830052, People's Republic of China.

Experimental Section

X-ray single crystal diffraction (SC-XRD)

All single-crystal X-ray diffraction data in the work were collected by using a Bruker D8 APEX-III diffractometer with Mo-Kα radiation (λ = 0.71073 Å) (operating at 50 kV and 1.4 mA). Refinement of single crystal data were solved and refined using SHELXT and OLEX 1.5 software packages, all non-hydrogen atoms are anisotropically manipulated. The drawing of $(IBA)_2SbBr_5$ and $(IBA)_6SbBr_6{\cdot}3Br$ were described using DIAMOND software. The crystal data (CCDC number: 2418065, 2418066, 2418067 and 2418068.) have been uploaded to the Crystallography data center in Cambridge (CCDC) in the work.

Synthesis of $(IBA)_2SbBr_5$ and $(IBA)_6SbBr_6{\cdot}3Br$

All the analytical grade reagents and solvents were purchased and used without further purification.

Isobutylamine (0.292 g, 4 mmol) and Sb_2O_3 (0.291 g, 1 mmol) were added to the solution of 36% HBr. Then it was stirred and filtered. The obtained yellow clear solution was placed in air for evaporation and crystallization, with the temperature maintained at 323 K. After approximately three days, block-shaped yellow crystals of the compound $(IBA)_2SbBr_5$ were obtained.

Isobutylamine (1.168 g, 16 mmol) and Sb_2O_3 (0.291 g, 1 mmol) were added to the solution of 36% HBr. Then it was stirred and filtered. The obtained yellow clear solution was placed in air for evaporation and crystallization, with the temperature maintained at 323 K. After approximately three days, block-shaped yellow crystals of the compound $(IBA)_6SbBr_6{\cdot}3Br$ were obtained.

Differential Scanning Calorimetry (DSC)

DSC measurement was performed on powder sample of $(IBA)_2SbBr_5$, and $(IBA)_6SbBr_6{\cdot}3Br$ by a NETZSCH-214 instrument. The sample was placed in aluminum crucible under nitrogen at atmospheric pressure. The experiment was conducted under nitrogen and atmospheric pressure, with heating and cooling rates of 10 $K{\cdot}min^{-1}$.

Dielectric Measurements

The dielectric response of $(IBA)_2SbBr_5$ and $(IBA)_6SbBr_6{\cdot}3Br$ was measured by a Tonghui TH2828A Precision LCR meter with the measuring AC voltage fixed at 1 V. The pressed-powder pellets with painted sliver glue were used as electrodes to test the dielectric constants within the frequency range of 0.5 kHz to 1 MHz.

Powder X-ray diffraction

Powder X-ray diffraction (PXRD) measurements were performed at room temperature on a Rigaku SmartLab SE X-ray diffractometer. The diffraction pattern is recorded at 2θ between 5 - 70° within the range, the step size is 0.02°.

UV-visible (UV-vis) Spectrophotometry.

UV-vis absorption spectra of these compounds were characterized using a Shimadzu UV-2600 spectrophotometry equipped with a xenon lamp as the excitation source at room temperature. The calculated optical bandgaps (E_g) are based on Tauc equation (1), where α is the absorption coefficient, h is Planck′ s constant, v is the frequency of vibration and A is the proportional constant. The value of the exponent n denotes the nature of the sample transition when n = 2 represents the indirect bandgap of semiconductors and n =1/2 represents the direct bandgap of semiconductors.

$(\alpha hv)^{1/n} = A(hv - Eg)$ (1)

Density Functional Theory (DFT) Calculations.

The band structure and partial density state were performed based on density function theory (DFT) by using the Vienna Ab-initio Simulation Package (VASP). Firstly, the crystallographic structures of compounds obtained from SC-XRD measurement were further optimized geometrically, employing the exchange-correlation interactions within the generalized gradient approximation (GGA) on the basis of the PerdewBurke-Ernzerh (PBE) function. Secondly, the band structure and partial density state of optimized structures were calculated by the PBE function with considering spin-orbit coupling (SOC) and without considering SOC, respectively. Meanwhile, the plane wave cut-off energy, the force and energy convergence criterions were set to be 520 eV, 0.02 eV/Å and 10^{-6} eV per atom, respectively. In addition, the other parameters and convergent criteria were the default values. Finally, the post-processing analysis was performed by using VASPKIT.

Table S1. Crystallographic data and structural refinement details of $(IBA)_2SbBr_5$ and $(IBA)_6SbBr_6{\cdot}3Br$.

	$(IBA)_2SbBr_5$		$(IBA)_6SbBr_6{\cdot}3Br$	
	LTP	HTP	LTP	HTP
Empirical formula	$C_8H_{24}Br_5N_2Sb$	$C_8H_{24}Br_5N_2Sb$	$C_{24}H_{72}Br_9N_6Sb$	$C_{24}H_{72}Br_9N_6Sb$
Formula weight	669.59	669.59	1285.81	1283.81
Temperature/K	299.0	340.0	293	343.0
Crystal system	monoclinic	orthorhombic	monoclinic	monoclinic
Space group	$P2_1/c$	$Cmce$	$I2/a$	$C2/c$
a/Å	13.003(4)	7.977(4)	10.4028(5)	10.441(5)
b/Å	20.473(5)	25.153(15)	20.5482(10)	20.603(11)
c/Å	7.940(2)	20.366(10)	23.4304(11)	25.590(14)
α/°	90	90	90	90
β/°	106.640(7)	90	92.013(4)	112.280(7)
γ/°	90	90	90	90
Volume/Å^3	2025.0(10)	4086(4)	5005.4(4)	5094(5)
Z	4	8	4	4
μ/mm^{-1}	2.196	11.114	7.756	7.622
F(000)	1248.0	2496.0	2496.0	2496.0
GoF on F^2	1.071	1.052	1.208	1.027
R_1 [I>=2σ (I)]	0.0742	0.0451	0.1224	0.0847
wR_2 [all data]	0.2437	0.1450	0.2146	0.3074

$$X(S_1)=\begin{bmatrix}0 & 0 & e_{13}\\ 0 & 0 & 0\\ e_{31} & 0 & 0\end{bmatrix} \qquad X(S_2)=\begin{bmatrix}0 & 0 & -e_{13}\\ 0 & 0 & 0\\ -e_{31} & 0 & 0\end{bmatrix}$$

where e_{13} and e_{31} represents the strains along the a-axis and c-axis of $(IBA)_2SbBr_5$. Based on the ferroelastic phase transition theory defined by Aizu, the spontaneous strains of $(IBA)_2SbBr_5$ was displayed equally in all the orientation states in the ferroelastic phase. But it will become zero when $(IBA)_2SbBr_5$ acts as the paraelastic phase. Therefore, so we calculated the spontaneous strains as follows:

$$e_{13}=e_{31}=e=\frac{1}{2}\left(\frac{7.94\times\cos 106.64}{25.153}\right)=-0.0451$$

$$X(S_2)=-\sqrt{2}e=0.0639$$

Hence, the spontaneous strain of $(IBA)_2SbBr_5$ as the ferroelastic phase is ≈0.0639.

The calculation details of distortion index

$$\Delta d = \frac{1}{6}\sum_{i=1}^{6}\frac{|d_i - d_{av}|}{d_{av}}$$

Where di represents each individual Sb Br bond length, d_{av} is the average bond length of all Sb-Br bonds in the [$SbBr_6$] octahedron.

Table S2. Selected bond lengths /Å and angles /° for $(IBA)_2SbBr_5$ at LTP.

Atom-Atom	Lengths /Å	Atom-Atom-Atom	Angle/˚
Sb1-Br1	2.6043(10)	Br1-Sb1-Br2	92.42(3)
Sb1-Br2	2.7727(10)	Br5-Sb1-Br4	89.19(3)
Sb1-Br3	2.7610(11)	Br1-Sb1-Br3	87.48(3)
Sb1-Br4	2.8572(11)	Br1-Sb1-Br4	89.98(4)
Sb1-Br5	2.8126(12)	Br1-Sb1-Br5	88.39(3)
N2-C5	1.466(13)	Br2-Sb1-Br4	177.27(3)
C5-C6	1.520(6)	Br2-Sb1-Br5	89.57(3)
C6-C7	1.551(7)	Br3-Sb1-Br2	87.90(3)
C6-C8	1.530(6)	Br3-Sb1-Br4	93.51(3)
N1-C1	1.463(14)	Br3-Sb1-Br5	175.06(3)
C1-C2	1.474(9)	N2-C5-C6	117.7(7)
C2-C3	1.549(15)	C5-C6-C7	105.8(5)
C2-C4	1.480(11)	C5-C6-C8	108.1(5)
		C8-C6-C7	105.2(5)
		N1-C1-C2	116.3(8)
		C1-C2-C3	109.1(8)
		C1-C2-C4	122.9(9)
		C4-C2-C3	118.9(8)

Table S3. Selected bond lengths /Å and angles /° for $(IBA)_2SbBr_5$ at HTP.

Atom-Atom	Lengths /Å	Atom-Atom-Atom	Angle/˚
Sb1-Br1	2.6661(14)	Br1-Sb1-$Br1^1$	93.70(7)
Sb1-$Br1^1$	2.6661(14)	Br1-Sb1-Br2	87.39(4)

Sb1-Br2	2.760(2)	Br1[1]-Sb1-Br2	87.39(4)
Sb1-Br3	3.0164(12)	Br1-Sb1-Br3	173.21(4)
Sb1-Br3[2]	3.0164(12)	Br1-Sb1-Br3[2]	91.63(5)
Sb1-Br4	2.805(2)	Br1[1]-Sb1-Br3	91.63(5)
N2-C5	1.486(10)	Br1[1]-Sb1-Br3[2]	173.21(4)
C5-C6	1.519(9)	Br1[1]-Sb1-Br4	89.03(4)
C5-C6	1.519(9)	Br1-Sb1-Br4	89.03(4)
C6-C7	1.540(8)	Br2-Sb1-Br3	97.07(5)
C6-C8	1.538(9)	Br2-Sb1-Br3[2]	97.07(5)
C1-N1	1.468(9)	Br2-Sb1-Br4	174.76(6)
C1-C2	1.536(10)	Br3-Sb1-Br3[2]	82.77(4)
C2-C3	1.525(9)	Br4-Sb1-Br3	86.85(5)
C2-C4	1.525(10)	Br4-Sb1-Br3[2]	86.85(5)
		Sb1[3]-Br3-Sb1	168.97(9)
		N2-C5-C6	112.8(9)
		N2-C5-C6	112.8(9)
		C6[1]-C5-C6	7(3)
		C5-C6-C7	106.8(15)
		C5-C6-C8	113.9(17)
		C8-C6-C7	100.2(18)
		N1-C1-C2	111.6(9)
		C3-C2-C1	116.5(17)
		C4-C2-C1	106.5(17)
		C4-C2-C3	112.6(18)

Symmetry codes: [1] 1-X, +Y, +Z; [2] 1/2+X, +Y, 1/2-Z; [3] -1/2+X, +Y, 1/2-Z

Table S4. Selected bond lengths /Å and angles /° for $(IBA)_6SbBr_6 \cdot 3Br$ at LTP.

Atom-Atom	Lengths /Å	Atom-Atom-Atom	Angle/˚
Sb1-Br1[1]	2.7978(15)	Br1[1]-Sb1-Br1	180
Sb1-Br1	2.7978(15)	Br1-Sb1-Br4[1]	90.27(5)

Sb1-Br4	2.8030(15)	Br1[1]-Sb1-Br4[1]	89.73(5)
Sb1-Br4[1]	2.8030(15)	Br1-Sb1-Br4	89.73(5)
Sb1-Br5[1]	2.8095(16)	Br1[1]-Sb1-Br4	90.27(5)
Sb1-Br5	2.8095(16)	Br1-Sb1-Br5	89.97(5)
N1-C1	1.497(10)	Br1[1]-Sb1-Br5	90.03(5)
N1-C11	1.42(4)	Br1[1]-Sb1-Br5[1]	89.97(5)
C1-C4	1.491(10)	Br1-Sb1-Br51	90.03(5)
C4-C11	1.489(10)	Br4-Sb1-Br4[1]	180
C4-C3	1.505(10)	Br4[1]-Sb1-Br5[1]	89.93(5)
C4-C13	1.503(10)	Br4-Sb1-Br5[1]	90.07(5)
C4-C7	1.502(10)	Br4[1]-Sb1-Br5	90.07(5)
C4-C15	1.495(10)	Br4-Sb1-Br5	89.93(5)
N3-C6	1.497(10)	Br5-Sb1-Br5[1]	180
N3-C2	1.500(10)	C4-C1-N1	122(2)
C6-C8	1.495(10)	C1-C4-C3	101(3)
C8-C2	1.486(10)	C1-C4-C15	166(3)
C8-C17	1.503(10)	C11-C4-C13	128(4)
C8-C9	1.500(10)	C11-C4-C7	107(3)
C8-C19	1.504(10)	C7-C4-C13	89.1(19)
C8-C5	1.501(10)	C15-C4-C3	89.4(19)
C10-N2	1.491(10)	C8-C6-N3	110(2)
C10-C16	1.489(10)	C6-C8-C17	111(3)
C12-N2	1.46(4)	C6-C8-C5	94.9(12)
C12-C16	1.492(10)	C2-C8-C9	128(3)
C14-C16	1.500(10)	C2-C8-C19	108(4)
C16-C18	1.497(10)	C9-C8-C19	86(3)
C16-C20	1.503(10)	C5-C8-C17	93.4(12)
C16-C21	1.496(10)	C16-C10-N2	117(2)
		N2-C12-C16	119(3)
		C10-C16-C18	118(3)

		C10-C16-C21	126(4)
		C12-C16-C14	135(4)
		C12-C16-C20	109(3)
		C14-C16-C20	93.4(12)
		C21-C16-C18	94.5(12)
		N1-C11-C4	128(3)
		C8-C2-N3	110(2)

Symmetry codes: [1] -1/2-X, 3/2-Y, 1/2-Z

Table S5. Selected bond lengths /Å and angles /° for $(IBA)_6SbBr_6 \cdot 3Br$ at HTP.

Atom-Atom	Lengths /Å	Atom-Atom-Atom	Angle/˚
Sb1-Br2	2.8128(13)	$Br2^1$-Sb1-Br2	180
Sb1-$Br2^1$	2.8128(13)	Br2-Sb1-Br4	90.12(3)
Sb1-$Br3^1$	2.8056(12)	$Br2^1$-Sb1-Br4	89.88(3)
Sb1-Br3	2.8056(12)	Br2-Sb1-$Br4^1$	89.88(3)
Sb1-$Br4^1$	2.8235(15)	$Br2^1$-Sb1-$Br4^1$	90.12(3)
Sb1-Br4	2.8235(15)	Br3-Sb1-$Br2^1$	90.21(4)
N7-C9	1.6902(12)	Br3-Sb1-Br2	89.79(4)
N8-CA	1.4794(10)	$Br3^1$-Sb1-Br2	90.21(4)
N9-C8	1.797(3)	$Br3^1$-Sb1-$Br2^1$	89.79(4)
CA-C2	1.5415(11)	Br3-Sb1-$Br3^1$	180.00(2)
C5-C8	1.501(3)	Br3-Sb1-$Br4^1$	89.95(4)
C5-C1	1.5144(17)	Br3-Sb1-Br4	90.05(4)
C5-C15	1.507(3)	$Br3^1$-Sb1-$Br4^1$	90.05(4)
C9-C14	1.4882(13)	$Br3^1$-Sb1-Br4	89.95(4)
C7-C14	1.5128(10)	$Br4^1$-Sb1-Br4	180
C14-C17	1.5274(14)	N8-CA-C2	114.43(4)
C2-C11	1.531(2)	C8-C5-C1	108.40(18)
C2-C12	1.5301(14)	C8-C5-C15	108.8(3)
		C15-C5-C1	108.1(2)

	C5-C8-N9	100.36(18)
	C14-C9-N7	105.92(6)
	C9-C14-C7	109.19(7)
	C9-C14-C17	108.40(5)
	C7-C14-C17	107.14(9)
	C11-C2-CA	105.54(11)
	C12-C2-CA	105.57(6)
	C12-C2-C11	106.10(16)

Symmetry codes: [1] 1/2-X, 1/2-Y, -Z

Table S6. PLQY reported in the literature

Compound	Dimension	PLQY (%)	Ref.
$(IBA)_6SbBr_6{\cdot}3Br$	0	10.22	This work
$(IBA)_2SbBr_5$	1	<1	This work
$(MTP)_2SbBr_5$	0	57	[1]
$H_3SbBr_6(L)_6$	0	55	[2]
$[TPPen]_2SbBr_5$	0	43.2	[3]
TPP_2SbBr_5	0	33	[4]
$[EtPPh_3]_2[SbBr_5]{\cdot}EtOH$	0	18.26	[5]
$[EtPPh_3]_2[SbBr_5]$	0	7.76	[5]
$(PMA)_3SbBr_6$	0	<1	[6]
$[HDBA]_2SbCl_5$	0	8.38	[7]
$[H_2ATMP]_2SbCl_7$	0	7.22	[7]
$[H_3PMDETA]\,Sb_2Cl_9$	1	2.11	[7]

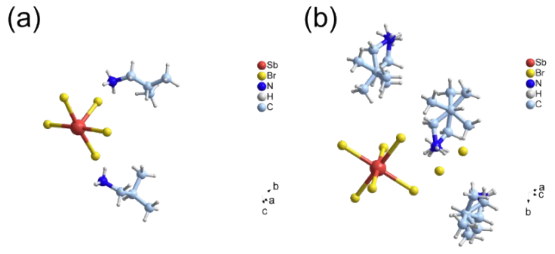

Fig. S1 (a)The asymmetric unit structure of $(IBA)_2SbBr_5$ and (b) $(IBA)_6SbBr_6{\cdot}3Br$.

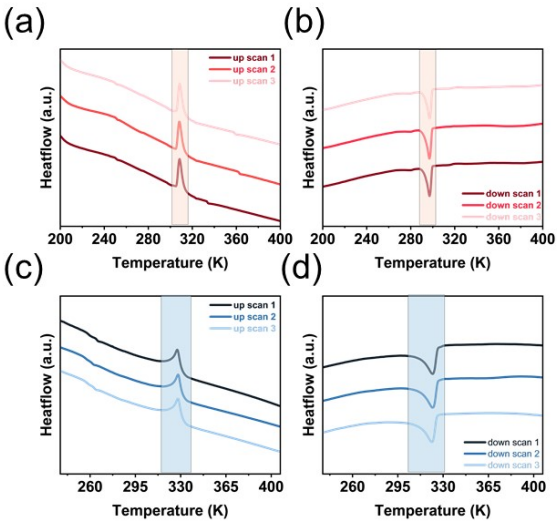

Fig. S2 The DSC up and down scans of $(IBA)_6SbBr_6{\cdot}3Br$ (a)(b) and $(IBA)_2SbBr_5$ (c)(d) for three crystals. (The three successive DSC curves were panned up and down for clarity.)

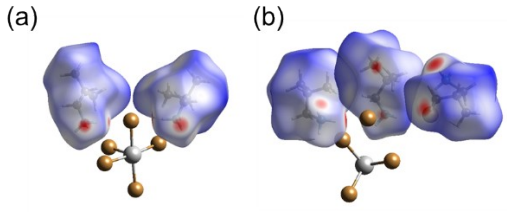

Fig. S3 The Hirshield surfaces of $(IBA)_2SbBr_5$ (a)and $(IBA)_6SbBr_6{\cdot}3Br$ (b).

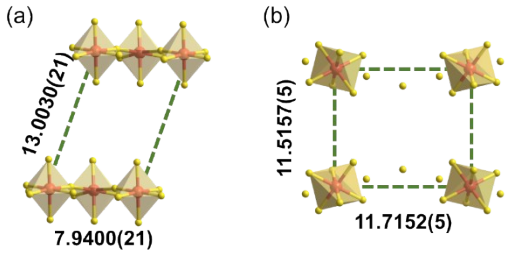

Fig. S4 The packing structures of $(IBA)_2SbBr_5$ (a) and $(IBA)_6SbBr_6{\cdot}3Br$ (b).

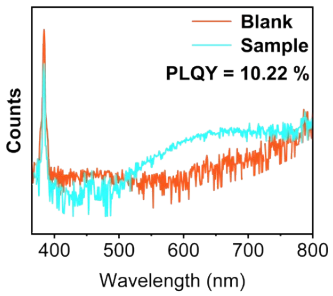

Fig. S5 Quantum yield of $(IBA)_6SbBr_6{\cdot}3Br$.

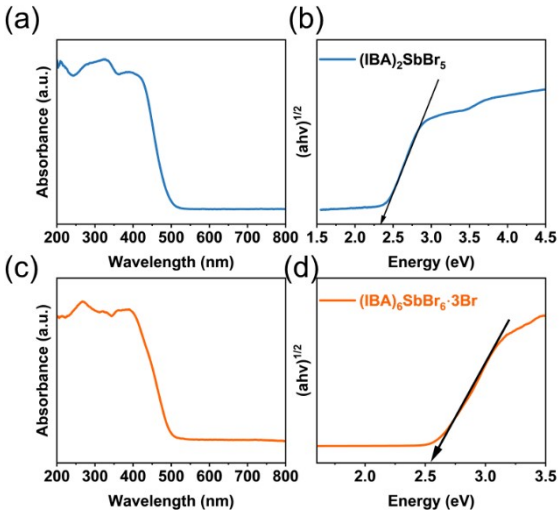

Fig. S6 UV-Vis absorption spectra and the band gaps of $(IBA)_2SbBr_5$ (a)(b) and $(IBA)_6SbBr_6{\cdot}3Br$ (c)(d).

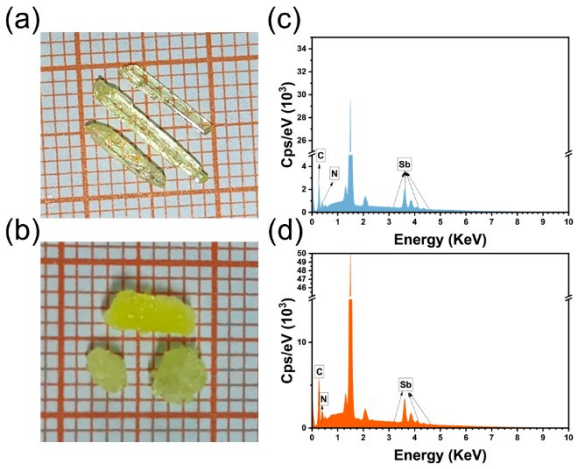

Fig**. S7** The Photographs of crystals $(IBA)_2SbBr_5$ (a) and $(IBA)_6SbBr_6{\cdot}3Br$ (b). The EDS Spectrogram of $(IBA)_2SbBr_5$ (c) and $(IBA)_6SbBr_6{\cdot}3Br$ (d).

References

1. B. Li, J. Jin, M. Yin, X. Zhang, M. S. Molokeev, Z. Xia and Y. Xu, Sequential and Reversible Phase Transformations in Zero-Dimensional Organic-Inorganic Hybrid Sb-based Halides towards Multiple Emissions, *Angew. Chem. Int. Ed.*, 2022, **61**, e202212741.
2. F. Lin, H. Wang, W. Liu and J. Li, Zero-dimensional ionic antimony halide inorganic–organic hybrid with strong greenish yellow emission, *J. Mater. Chem. C*, 2020, **8**, 7300-7303.

3. J. Jin, S. Geng, K. Han, Z. Xiao and Z. Xia, Blue-Light-Excitable Red-to-Near Infrared Photoluminescence in 0D Antimony(III) Bromide Hybrids for Supplemental Lighting, *Adv. Opt. Mater.*, 2024, **12**, 2303178.
4. V. Morad, S. Yakunin, B. M. Benin, Y. Shynkarenko, M. J. Grotevent, I. Shorubalko, S. C. Boehme and M. V. Kovalenko, Hybrid 0D Antimony Halides as Air-Stable Luminophores for High-Spatial-Resolution Remote Thermography, *Adv. Mater.*, 2021, **33**, 2007355.
5. Y.-C. Peng, S.-H. Zhou, J.-C. Jin, Q. Gu, T.-H. Zhuang, L.-K. Gong, Z.-P. Wang, K.-Z. Du and X.-Y. Huang, Nearly one-fold enhancement in photoluminescence quantum yield for isostructural zero-dimensional hybrid antimony(iii) bromides by supramolecular interaction adjustments, *Dalton Trans.*, 2022, **51**, 4919-4926.
6. D. Chen, F. Dai, S. Hao, G. Zhou, Q. Liu, C. Wolverton, J. Zhao and Z. Xia, Crystal structure and luminescence properties of lead-free metal halides (C6H5CH2NH3)3MBr6 (M = Bi and Sb), *J. Mater. Chem. C*, 2020, **8**, 7322-7329.
7. Y.-Y. Ma, H.-M. Pan, D.-Y. Li, Y.-H. Liu, T. Lu, X.-W. Lei and Z. Jing, Structural evolution and photoluminescence properties of hybrid antimony halides, *J. Solid State Chem.*, 2022, **314**, 123404.